

RESEARCH ARTICLE

Specialization for rapid excitation in fast squid tentacle muscle involves action potentials absent in slow arm muscle

William F. Gilly¹, Corbin Renken^{2,*}, Joshua J. C. Rosenthal² and William M. Kier^{3,†}

ABSTRACT

An important aspect of the performance of many fast muscle fiber types is rapid excitation. Previous research on the cross-striated muscle fibers responsible for the rapid tentacle strike in squid has revealed the specializations responsible for high shortening velocity, but little is known about excitation of these fibers. Conventional whole-cell patch recordings were made from tentacle fibers and the slower obliquely striated muscle fibers of the arms. The fast-contracting tentacle fibers show an approximately 10-fold greater sodium conductance than that of the arm fibers and, unlike the arm fibers, the tentacle muscle fibers produce action potentials. *In situ* hybridization using an antisense probe to the voltage-dependent sodium channel present in this squid genus shows prominent expression of sodium channel mRNA in tentacle fibers but undetectable expression in arm fibers. Production of action potentials by tentacle muscle fibers and their absence in arm fibers is likely responsible for the previously reported greater twitch–tetanus ratio in the tentacle versus the arm fibers. During the rapid tentacle strike, a few closely spaced action potentials would result in maximal activation of transverse tentacle muscle. Activation of the slower transverse muscle fibers in the arms would require summation of excitatory postsynaptic potentials over a longer time, allowing the precise modulation of force required for supporting slower movements of the arms.

KEY WORDS: Calcium current, Cephalopod muscle, Current clamp, Patch clamp, Sodium current, Voltage clamp

INTRODUCTION

Contractile properties of muscle fibers, including maximum tension, shortening velocity, twitch duration and/or endurance, vary widely, often within an individual organism, and reflect specialization for a given muscle fiber's specific role in locomotion, movement or postural support. Mechanisms of muscle specialization that provide the remarkable range of performance observed have been well studied in vertebrates and some arthropods but less so in soft-bodied invertebrates. Recent work (reviewed below) on the transverse muscle fibers of the tentacles of squid has revealed mechanisms for achieving high shortening velocity that differ from those described previously for vertebrate muscle (Kier,

1991; Kier and Schachat, 1992, 2008; Shaffer and Kier, 2012, 2016). We know relatively little, however, about how excitation, another important functional property, is achieved in these fibers and many other types of rapidly contracting muscle fibers.

During prey capture by the squid *Doryteuthis pealeii*, the animal first orients towards the prey, approaches slowly to within about one mantle length (ML), and then finally lunges forward a short distance ($\sim 1/2$ ML) while the two tentacles rapidly elongate to strike the prey with terminal portions called clubs (Kier and Van Leeuwen, 1997). Suckers on the clubs adhere to the prey, and the tentacles then retract, bringing the prey into the grasp of the eight non-extensible arms that subdue and manipulate the prey through slower bending and torsional movements. Tentacle elongation of nearly 80% occurs in only 20–40 ms with a peak strain rate of $23\text{--}43\text{ s}^{-1}$, peak velocity of approximately 2 m s^{-1} and peak acceleration of 250 m s^{-2} at 19°C (Kier and Van Leeuwen, 1997). These values are among the highest observed for animal movement that does not rely on elastic energy-storage mechanisms for power amplification (Patek, 2015). The musculature responsible for rapid tentacular extension is the transverse muscle mass, composed of cross-striated fibers. In contrast, the transverse muscle mass of the arms, composed of obliquely striated fibers, supports the slower bending and torsional movements (but not significant extension) used in prey handling and other behaviors (Kier, 1982).


Contractile properties of these two muscle masses reflect their different roles. Unloaded shortening velocity of transverse tentacle fibers (>15 muscle lengths s^{-1}) is 10-fold faster than that of transverse arm fibers based on experiments using isotonic shortening, and time to peak force development (~ 35 ms) in isometric contractions is about half as long. The relationship between these two types of muscle fibers is of considerable interest, because the obliquely striated fibers represent the developmental and likely evolutionary precursor of the fast tentacle fibers (Kier, 1996). Thus, these fiber types represent an ideal system to explore the mechanisms of specialization for rapid excitation in a highly mobile but soft-bodied mollusk.

Although contractile properties in vertebrate skeletal muscle are associated with different isoforms of contractile proteins to a large degree, specialization for fast contraction in transverse tentacle versus arm muscle fibers in squid primarily involves structural specializations. Few differences are observed in the biochemistry of the myofilament lattice (Kier and Schachat, 1992, 2008), and the nucleotide and amino acid sequences of the myosin heavy chain are identical (Shaffer and Kier, 2012, 2016). Instead, specialization involves ultrastructural differences in the arrangement and dimensions of the myofilaments. Tentacle fibers exhibit cross-striation with unusually short thick filaments ($\sim 0.8\text{ }\mu\text{m}$ in *D. pealeii*) and thus differ from the arm fibers, which like most cephalopod muscle fibers are obliquely striated and have long thick filaments ($\sim 7.5\text{ }\mu\text{m}$ in *D. pealeii*) (Kier, 1985, 1991, 2016). Because shorter thick filaments result in more elements in series

¹Hopkins Marine Station of Stanford University, 120 Ocean View Boulevard, Pacific Grove, CA 93950, USA. ²The Eugene Bell Center, Marine Biological Laboratory, Woods Hole, MA 02543, USA. ³Department of Biology, CB# 3280 Coker Hall, University of North Carolina, Chapel Hill, NC 27599, USA.

*Present address: Yale University School of Medicine, 333 Cedar Street, New Haven, CT 06510, USA.

†Author for correspondence (billkier@bio.unc.edu)

 C.R., 0000-0001-7015-1312; W.M.K., 0000-0003-1404-8657

List of symbols and abbreviations

C_{in}	cell input capacitance
DEPC	diethylpyrocarbonate
dV/dt fall	maximum negative rate of voltage change
dV/dt rise	maximum positive rate of voltage change
EPSP	excitatory post-synaptic potential
G_K	potassium conductance
$G_{max-fit}$	maximal conductance fitted to a sigmoid curve
$G_{max-slope}$	maximal slope conductance
G_{Na}	sodium conductance
I_{Ca}	calcium current
I_K	potassium current
I_{Na}	sodium current
k	steepness factor
PBS	phosphate-buffered saline
R_{in}	input resistance
R_s	series resistance
SSC	saline–sodium citrate
$t_{1/2on}$	time to half-peak current
TTX	tetrodotoxin
V	membrane voltage
V_K	reversal potential for potassium current
V_{Na}	reversal potential for sodium current
V_p	pipette command voltage
V_{pre}	prepulse voltage
$V_{1/2}$	voltage at half-activation
$\tau_{inactivation}$	inactivation time constant
τ_{off}	deactivation (channel closing) time constant
τ_{on}	activation (channel opening) time constant

(per unit length), and the shortening velocity of elements in series is additive, this ultrastructural difference is responsible for the 10-fold greater shortening velocity of tentacle versus arm fibers (Kier, 1985; Kier and Curtin, 2002; Van Leeuwen and Kier, 1997).

Another important difference between transverse muscle fibers of tentacles and arms is that the ratio of twitch force to peak tetanic force is 0.66 in tentacle fibers versus 0.03 in arm fibers (Kier and Curtin, 2002). Structural mechanisms cannot explain this 20-fold difference in twitch-to-tetanus ratio. Because effective prey capture with the tentacles is associated with explosive force development (Van Leeuwen and Kier, 1997), we hypothesized that excitation of tentacle fibers would be characterized by an all-or-nothing type of

electrical excitability based on an action potential, similar to the system in vertebrate skeletal muscle. In contrast, we hypothesized that the slower bending and torsional movements of arms would be associated with a graded type of activation that does not involve action potentials, a character more typically found in invertebrate muscle (Hoyle, 1969; Zachar, 1971) or with an excitability mechanism based on slower, Ca-based action potentials as has been demonstrated in octopus arm muscle (Rokni and Hochner, 2002; Neshet et al., 2019). The present study tested these hypotheses using whole-cell patch-clamp methods with enzymatically dissociated muscle fibers of each type to carry out voltage- and current-clamp recordings and with *in situ* hybridization techniques to provide a molecular identification of mRNA encoding a squid Na_v protein in both types of tissues. Both approaches are consistent with the idea that tentacle fibers express voltage-gated Na channels at a much higher level than do arm fibers, and that tentacular excitation depends on an action potential based on Na influx.

MATERIALS AND METHODS

Animals and tissues

Specimens of the California market squid [*Doryteuthis opalescens* (Berry 1911)] were captured by jigging off Pacific Grove, CA, USA, and transported in an aerated holding tank to Hopkins Marine Station of Stanford University, Pacific Grove, CA, USA, where they were maintained in a flow-through seawater system at ambient temperature (13–16°C). Animals were killed by rapid decapitation, and the tentacles and ventral-most 4th pair of arms were removed and placed in filtered seawater. Cross-sectional slices approximately 2 mm thick were cut from the mid-region of the tentacular stalk and the arm with a broken double-edge razor blade on a Sylgard surface. Portions of the transverse muscle mass were dissected from the slice, being careful to exclude all other muscle fiber orientations and the axial nerve cord (Fig. 1). Slices were prepared from the arms in the same manner. Slices from tentacles and arms were used to prepare cells for electrophysiology as described below.

Specimens of the longfin inshore squid [*Doryteuthis pealeii* (Lesueur 1821)] were collected by otter trawl in Vineyard Sound close to Menemsha, Martha's Vineyard, by the Marine Biological Laboratory, Woods Hole, MA, USA. Because the *in situ*

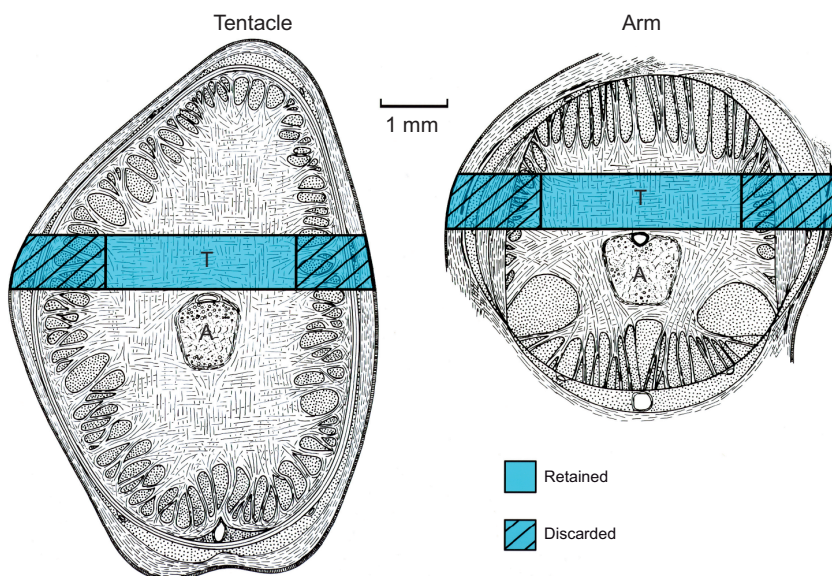


Fig. 1. Diagram of transverse sections of the tentacle and arm of the squid *Doryteuthis* spp. showing the portion of transverse muscle mass sampled. The transverse muscle mass (T) occupies the bulk of the core region surrounding the axial nerve cord (A) in both tentacle and arm. Samples that included transverse muscle fibers only were obtained by removing a slice (blue shaded portion) from a transverse section and then cutting and discarding the ends of the slice (hatched regions). After Kier and Curtin (2002).

hybridization experiments were performed in Woods Hole, this locally occurring species was used. The same differences in the transverse muscle of the arms and tentacles have been observed not only in different species of the genus *Doryteuthis* (Suborder Myopsina) but also in a different genus, *Illex illecebrosus*, from a separate suborder (Oegopsina) (Kier, 1985). Indeed, the same difference in transverse muscle between the arms and tentacles has been found in the cuttlefish *Sepia officinalis*, a member of a separate order (Sepiida) from the squids (Teuthida) (Shaffer and Kier, 2016). Animals were transported to holding tanks in the Marine Biological Laboratory with flowing seawater. After holding for 1–3 days, specimens were killed by rapid decapitation and 1 cm sections of arm and tentacle were dissected and prepared as described in the *in situ* hybridization section below.

Tissue preparation and cell dissociation for electrophysiology

Tissue samples from arms and tentacles were separately incubated in 5 mg ml⁻¹ collagenase (Gibco, Type 1) in low-Ca artificial seawater composed of (in mmol l⁻¹): 480 NaCl, 2 CaCl₂, 25 MgCl₂, 25 MgSO₄, 10 Hepes (pH 7.8) for 2–2.5 h at room temperature. Tissue pieces were then moved using a 200 µl micropipette to a sterile 35 mm polystyrene culture dish (Falcon 353001, Corning, New York, NY, USA) with a Perspex ring insert (1 cm diameter hole) attached to the bottom of the dish with petroleum jelly (Vaseline, Unilever, London, UK) or silicone vacuum grease (Dow Corning, Midland, MI, USA). The central well for tissue deposition (0.5 ml volume) contained culture medium consisting of Liebovitz's L-15 (Gibco, Inc., Dublin, Ireland) supplemented with the following salts to achieve approximate osmotic balance with seawater (in mmol l⁻¹): 263 NaCl, 4.6 KCl, 25 MgCl₂, 25 MgSO₄ plus 3.5 EGTA (to achieve a final Ca²⁺ concentration of ~0.2 mmol l⁻¹), 2 Hepes (pH 7.8), 5 trehalose, plus 50 IU ml⁻¹ penicillin and 0.05 mg ml⁻¹ streptomycin. Tissue fragments were triturated 2–4 times using the transfer micropipette, and the cells were allowed to settle for ~1 h before transferring the dish to an incubator maintained at 16°C. Cylindrical muscle cell fragments were used for electrophysiological experiments within 36 h of initial incubation.

Whole-cell recordings

Conventional whole-cell patch recordings were carried out in both voltage- and current-clamp mode with a List EPC-7 amplifier (Adams & List Assoc., Great Neck, NY, USA) and pCLAMP 9 data acquisition (Molecular Devices, L.L.C., San Jose, CA, USA). Holding potential was -70 or -80 mV. Control pulses to remove linear ionic and capacity currents (P/4 or P/-4) were delivered from -80 mV. Electrodes generally had resistances of <3 MΩ before attaching to a cell, and electronic series resistance compensation was employed to the maximum extent possible during whole-cell recordings, generally 50–70%. Muscle 'fibers' isolated from both tentacles and arms were generally <40 µm in length and ~7 µm in diameter, and input capacitance ranged from 5 to 30 pF (measured with a 10 mV voltage step; see Armstrong and Gilly, 1992). Fibers of this size showed no slow component of capacity current, consistent with good spatial control of voltage. In a few fibers, 'escape' from voltage-clamp control was evident as a result of the combination of high electrode resistance and large sodium current (*I*_{Na}) in fibers with a low concentration of internal Na (0 mmol l⁻¹, see below), and data from such fibers were excluded from further analysis. All recordings were carried out at 15–16°C, the ambient environmental water temperature in Monterey Bay.

For recording *I*_{Na} in isolation from potassium current (*I*_K), the external (bath) solution contained (in mmol l⁻¹): 480 NaCl, 10 CaCl₂, 25 MgCl₂, 25 MgSO₄, 10 Hepes (pH 7.8), and the internal (pipette) solution contained (in mmol l⁻¹): 50 NaCl, 50 NaF, 120 sodium glutamate, 25 TEA Cl, 381 glycine, 1 EGTA, 1 EDTA, 300 sucrose, 10 Hepes (pH 7.8). These K-free solutions ('480Na/220Na') were used to study 12 tentacle fibers and 7 arm fibers.

For recording *I*_K (or *I*_{Na}+*I*_K), the same external solution was used with 20 mmol l⁻¹ NaCl replaced by 20 mmol l⁻¹ KCl, and the internal solution contained (in mmol l⁻¹): 20 KCl, 50 KF, 230 potassium glutamate, 130 glycine, 1 EGTA, 1 EDTA, 290 sucrose, 10 Hepes (pH 7.8). These solutions ('460Na/300K') were used to study 20 tentacle and 13 arm fibers.

Sodium conductance (*G*_{Na}) was estimated based on peak *I*_{Na}-voltage relationships: $G_{Na} = I_{Na} / (V - V_{Na})$, where *V* is membrane voltage after correcting the pipette command voltage (*V*_p) for series resistance (*R*_s) error ($V = V_p - I_{Na} \times R_s$), and *V*_{Na} is the reversal potential for *I*_{Na} (Armstrong and Gilly, 1992). Maximal *G*_{Na} (normalized by cell input capacitance, *C*_{in}) was estimated in two ways. (1) A straight line was fitted to the linear portion of the *I*_{Na}-*V* relationship around *V*_{Na}; with the solutions used, this maximal slope conductance (*G*_{max-slope}) is equivalent to the maximum chord conductance as defined above. (2) A sigmoid curve was fitted to the *G*_{Na}-*V* relationship:

$$G_{Na} = G_{\max-fit} [1 + \exp(V_{1/2} - V)/k], \quad (1)$$

where *G*_{max-fit} is maximal *G*_{Na}, *V*_{1/2} is the voltage where *G*_{Na}=0.5*G*_{max-fit}, and *k* is a steepness factor (e-fold change in *k* mV). These methods generally gave nearly identical values for maximal *G*_{Na}. Fitting was done using IGOR Pro V6.3.7.3 (Wavemetrics, Lake Oswego, OR, USA).

Potassium conductance (*G*_K) was estimated from the peak *I*_K-*V* relationship as $G_K = I_K / (V - V_K)$, where *V* is membrane voltage after correcting for *R*_s error (see above), and *V*_K is the measured reversal potential of *I*_K 'tail' currents between -100 and -30 mV following an activating pulse of 5 ms duration to +40 mV. *V*_K in the solutions used for *I*_K measurements was -53.1±2.5 mV (mean±s.d., *n*=13 tentacles) and -56.6±6.3 mV (*n*=12 arms). The *G*_K-*V* relationship was fitted to a sigmoid curve (analogous to Eqn 1) to yield estimates of *G*_{max-fit}, *V*_{1/2} and *k* for *G*_K.

In general, *I*_{Na} and *I*_K were the only voltage-dependent currents observed in both tentacle and arm fibers. In experiments that employed K-containing solutions, separation of peak inward *I*_{Na} from *I*_K was possible, because *I*_{Na} activated much more rapidly, but contamination by *I*_K undoubtedly led to an underestimate of *I*_{Na} amplitude at positive voltages, particularly in arm fibers where *I*_{Na} was small. *G*_{Na} was significantly larger in arm fibers studied in K-free solutions versus K-containing ones (*P*<0.01 by 2-tailed *t*-test; see Table S1), but the difference was not significant for tentacle fibers.

In several tentacle fibers (4 of 31 total), non-inactivating inward current, presumably calcium current (*I*_{Ca}), of significant amplitude in relation to *I*_{Na} was observed (26±12% of peak inward current; mean±s.d.). Activation of this putative *I*_{Ca} was distinctly slower than that of *I*_{Na}, *I*_{Ca} did not show a reversal potential at positive voltages in K-free solutions, and tetrodotoxin (TTX, 200 nmol l⁻¹) eliminated *I*_{Na} but had no effect on *I*_{Ca}. In two of these fibers, *I*_{Ca} 'ran down' during the experiment, and *I*_{Na} could then be determined without contamination. In the other two fibers, a prepulse procedure (see Fig. 2) allowed adequate separation of *I*_{Na}. Data from these cells were included in the tabulation of *G*_{Na} and *G*_K properties (Table S1).

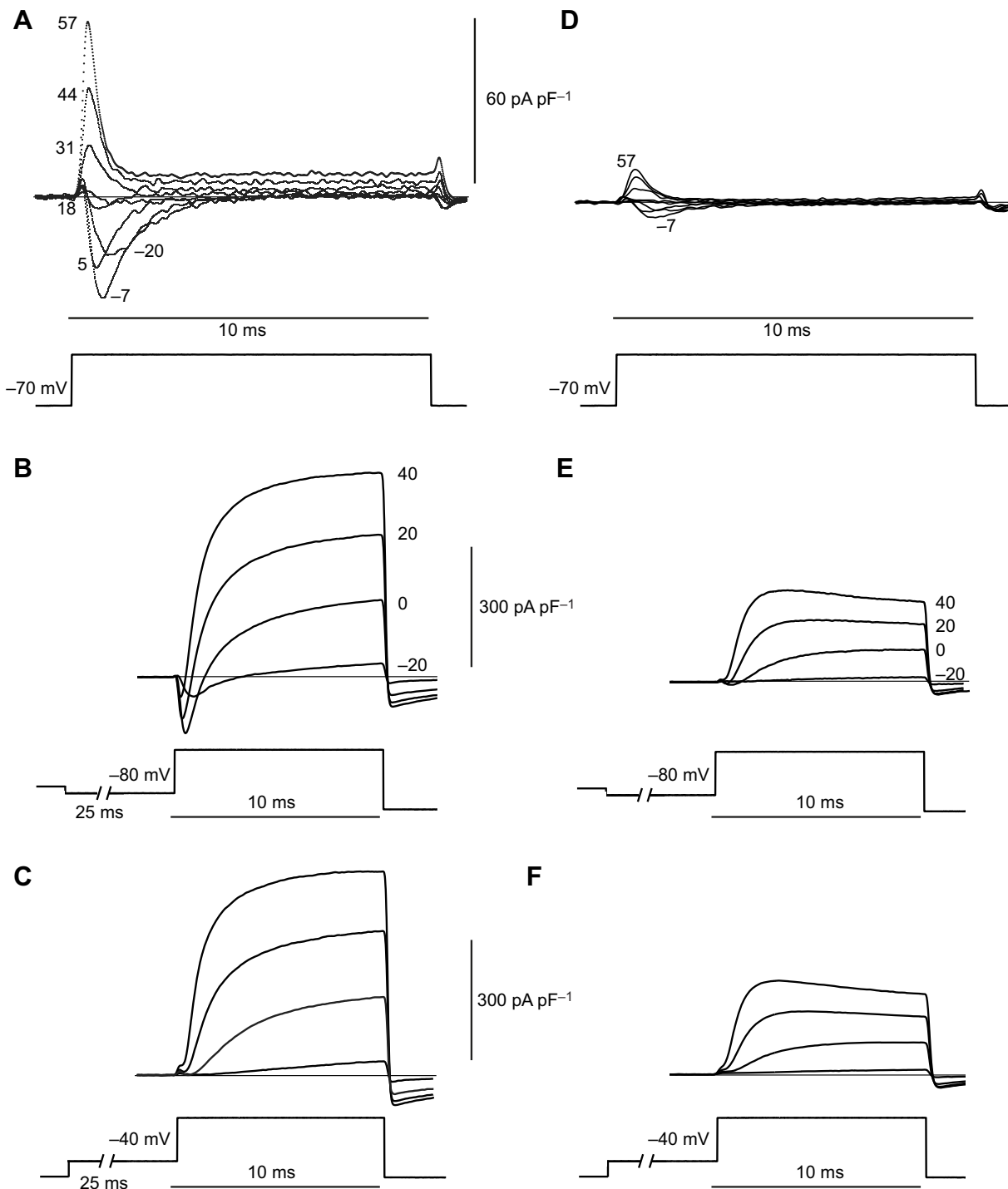


Fig. 2. Sodium and potassium current (I_{Na} and I_K) in transverse tentacle and arm fibers of squid. (A) Inward and outward I_{Na} recorded in K-free solutions from a transverse tentacle fiber at the indicated voltages (mV) (fiber ID: JUL2017G). (B) Inward I_{Na} and outward I_K recorded from a tentacle fiber at the indicated voltages (mV) (JUL2017C). (C) Recordings from the same fiber (at the same voltages) following a prepulse to -40 mV to inactivate I_{Na} . (D) I_{Na} recorded from a transverse arm fiber at the same voltages as those indicated in A (JUL2117A). (E) I_{Na} and I_K recorded from a transverse arm fiber at the indicated voltages (mV) (JUL1917B). (F) Recordings from the same fiber (at the same voltages) following a prepulse to -40 mV to inactivate I_{Na} . Vertical scale bars apply to panels on both left and right.

In one other tentacle fiber and in one arm fiber (of 20 total), peak I_{Ca} exceeded peak I_{Na} , and it was not possible to isolate I_{Na} reliably. Data from these two fibers were excluded from tabulation in Table S1.

Current-clamp recordings employed the same solutions as those used for measuring I_K (and $I_{Na}+I_K$) in voltage-clamp experiments.

A cell was studied first under voltage clamp, and passive electrical properties [input resistance (R_{in}), C_{in} , R_s] and I_{Na} and I_K were documented. Current clamp was then activated with the resting potential manually set to -70 mV. A series of negative and positive current pulses were then delivered, and membrane voltage changes were recorded. Positive stimuli were increased in

amplitude until the action potential rate of rise appeared to reach a limit.

Maximum rates of rise (dV/dt rise) and fall (dV/dt fall) of action potentials were measured from the time derivative of the voltage change in response to a depolarizing current. Pulse durations for tentacle fibers were 2–10 ms; those for arm fibers were 5–20 ms. The maximal value of dV/dt rise thus determined was corrected (dV/dt rise*) for contamination by the passive response due to the depolarizing stimulus by subtracting a ‘baseline’ value, with the baseline value set equal to dV/dt immediately preceding the positive inflection associated with the action potential. This procedure was straightforward with tentacle fibers, in which a positive inflection was always evident, but the lack of a distinct inflection in the case of arm fibers resulted in values of dV/dt rise* that were essentially zero. Responses to the strongest 2–3 stimuli in each muscle fiber were analyzed, and the measured rates were averaged for that fiber.

In situ hybridizations

Sample preparation

Freshly dissected tissue samples of arms and tentacles were fixed overnight at 4°C in 4% paraformaldehyde (Electron Microscopy Sciences, Hatfield, PA, USA) in filtered seawater with gentle rocking. Fixed tissues were washed 3 times in phosphate-buffered saline (PBS) treated with diethylpyrocarbonate (DEPC), dehydrated in a graded series of methanol and stored at –20°C. After washing 3 times in 100% ethanol, tissues were cleared at room temperature by washing 5 times for 20 min each with HistoSol (National Diagnostics, Atlanta, GA, USA) and then infiltrated stepwise with Paraplast Plus paraffin wax (Leica Biosystems, Buffalo Grove, IL, USA) at 60°C in successive washes overnight and the following day. Paraffin-infiltrated specimens were embedded in standard histology molds and allowed to harden for 24 h before sectioning at 5–8 µm on a rotary microtome. Sections were adhered to charged microscope slides (Fisher Scientific, Pittsburgh, PA, USA) and allowed to dry overnight before use.

Probe synthesis

A 701 bp portion of the *D. pealeii* voltage-dependent Na channel (nt 2582–3282; Rosenthal and Gilly, 1993; Alon et al., 2015) was amplified by PCR from stellate ganglion cDNA using the forward primer 5' TCAGTATTGTGCGCAGGGACGATGGG 3' and the reverse primer 5' **AGTAATACGACTCACTATAGGGAGAAT-CCCCACTTCGCTGGCAAGAC** 3' (nucleotides in bold are a T7 RNA polymerase promoter tag). The identity between the *D. pealeii* and *D. opalescens* open reading frames is 97.9% so the probe would be expected to bind to each equally. A MEGAscript™ T7 Transcription Kit (Invitrogen, Dublin, Ireland) was used with a 3:1 ratio of UTP to digoxigenin-11-UTP (Roche, Indianapolis, IN, USA) to transcribe antisense RNA. The transcription product was diluted in hybridization solution (O'Neill et al., 2007) and used as the experimental probe in subsequent *in situ* hybridization experiments.

A sense probe to the 3' UTR of the *Xenopus laevis insm2* mRNA was used as a negative control. This clone contains nt 2465–4764 of *insm2*, cloned into the EcoRI site of the PCR II vector (Invitrogen) with a 5' GCCCTT extension and a 3' TAAGGGC extension. It was linearized by digestion with XhoI, and then used as a template for RNA synthesis using the MEGAscript™ SP6 Transcription Kit (Invitrogen). A 3:1 ratio of UTP to digoxigenin-11-UTP (catalog number 11209256910, Roche) was used for transcription. The 2421 bp transcription product was diluted in hybridization solution

and used as a control probe to assess non-specific binding in subsequent *in situ* hybridization experiments.

Hybridizations

In situ hybridizations were performed as described by O'Neill et al. (2007) with the following modifications. After deparaffinizing slides 2×5 min in HistoSol, slides were rinsed 2×5 min in 100% ethanol and rehydrated stepwise with 2 min rinses in PBS treated with 0.1% DEPC (10%, 30%, 50% DEPC-treated PBS/ethanol), DEPC-treated water, DEPC-treated PBS+0.1% Tween, and then 2× in saline–sodium citrate (SSC) buffer. Rehydrated slides were then hybridized with 250 µl of probe (1 ng µl⁻¹) in hybridization solution under glass cover slips overnight at 68°C in chambers humidified with 2× SSC. Subsequent washes, blocking, incubation and staining were performed as described by O'Neill et al. (2007), except overnight incubation with 1:2000 anti-digoxigenin-AP antibody (catalog number 11093274910, Roche) was performed at room temperature, and the coloring reaction was initiated with BM Purple (catalog number 11442074001, Roche). After staining for a total of 185 h at room temperature and 81 h at 4°C, slides were washed 10 min in PBS, post-fixed for 20 min with 4% paraformaldehyde in PBS, rinsed in PBS and mounted with Fluoromount G (SouthernBiotech, Birmingham, AL, USA).

Microscopy and image processing

Mounted slides were imaged on a Zeiss Observer microscope using the tilescan function with 10× and 20× objectives. All images were captured in one session using identical intensity and exposure settings to ensure consistency between samples. Overlapping images from tilescans were stitched together, rotated and cropped using Zen Blue software (Zeiss, Oberkochen, Germany). Identical non-linear gamma adjustments to optimize white and black points were also performed consistently across all images in Zen Blue. Images were then Gaussian downsampled to 300 dpi using the ‘downsample’ plugin in Fiji (Schindelin et al., 2012) and assembled into panels with Adobe Illustrator CS5 (Adobe, San Jose, CA, USA).

RESULTS

Voltage-dependent Na conductance in transverse muscle fibers from tentacle versus arm

Voltage-clamp measurements demonstrated the existence of voltage-dependent I_{Na} (Fig. 2A) and I_K (Fig. 2B) in every transverse tentacle muscle fiber studied. An inactivating prepulse (–40 mV for 25 ms) completely eliminated I_{Na} with relatively little effect on I_K (Fig. 2C), and I_{Na} was reversibly eliminated by 200 nmol l⁻¹ tetrodotoxin (TTX; not illustrated). In contrast, arm muscle fibers showed much less (or no) I_{Na} (Fig. 2D) as well as smaller I_K (Fig. 2E,F) when normalized by cell capacitance.

In some tentacle fibers, records were obtained in K-free solutions without (Fig. 3A) and with (Fig. 3B) an inactivating prepulse in order to identify prepulse-sensitive I_{Na} (Fig. 3C). G_{Na} was derived from peak I_{Na} measured at each voltage (V) and the measured reversal potential (V_{Na} ; Fig. 3D) as described in Materials and Methods. Maximum G_{Na} was estimated from the maximal slope of the I_{Na} – V relationship at positive voltages ($G_{max-slope}$) (Fig. 3D) and from the sigmoid curve fit to the G_{Na} – V relationship ($G_{max-fit}$, $V_{1/2}$, k ; Fig. 3E) as described in Materials and Methods. Parameters describing G_{Na} were not significantly different in tentacle fibers studied with ($n=4$) or without ($n=7$) a prepulse as indicated in Table S1. Corresponding data for transverse arm fibers (records in Fig. 2D) are included in Fig. 3D,E.

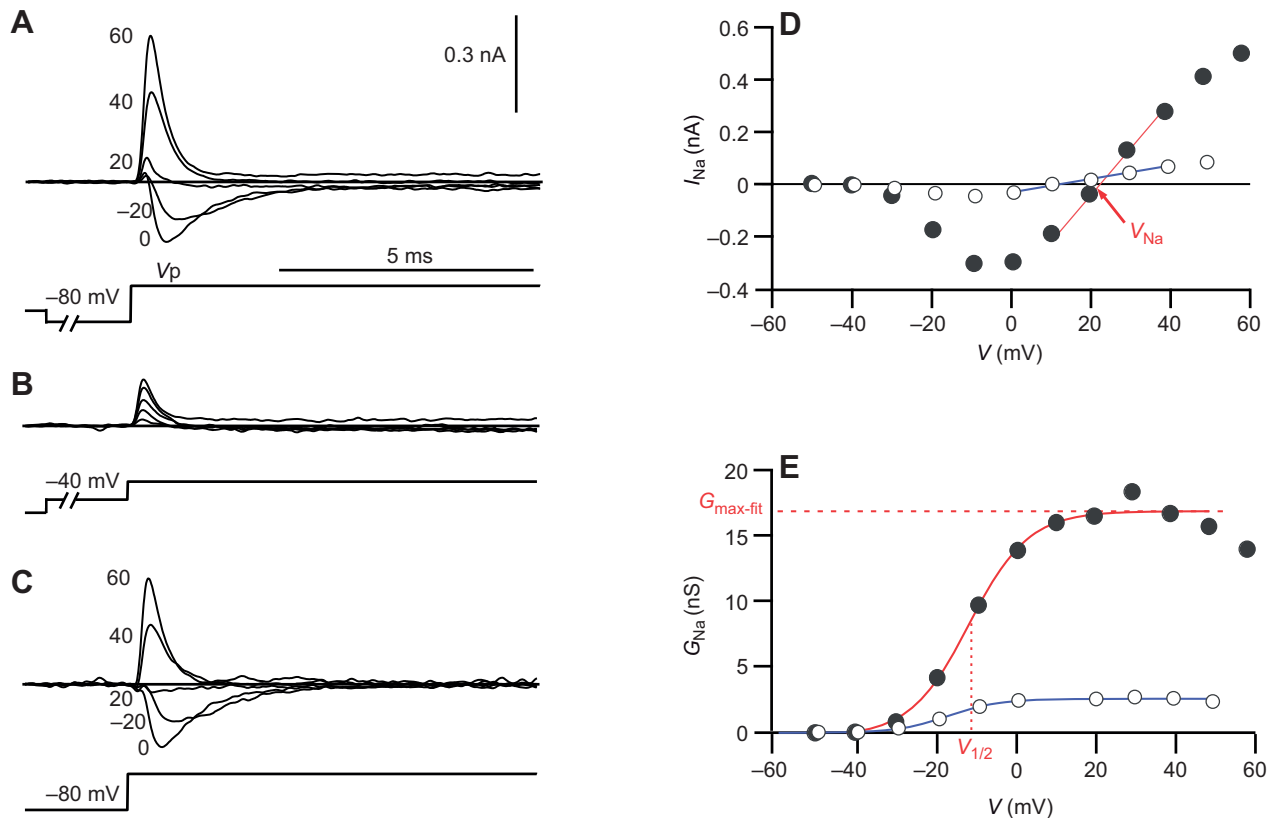


Fig. 3. Properties of prepulse-sensitive I_{Na} in a transverse tentacle fiber. (A) Inward and outward I_{Na} recorded in K-free solutions at the indicated voltages (mV). V_p , pipette command voltage. (B) Currents recorded with a 25 ms prepulse to -40 mV to inactivate I_{Na} . Residual currents are due to imperfect subtraction of the capacity transient using the P/4 procedure (see Materials and Methods). (C) Prepulse-sensitive I_{Na} obtained by subtraction of records in B from those in A. (D) Peak (prepulse-sensitive) I_{Na} versus voltage corrected for series resistance (R_s) error at the time of peak current (filled circles). The solid red line represents a linear fit used to determine peak sodium conductance (G_{Na}) from the slope ($G_{max-slope}=1.99$ nS pF $^{-1}$) and reversal potential ($V_{Na}=22.6$ mV, arrow). (E) The relationship between G_{Na} and V was fitted with a sigmoid curve to determine properties of G_{Na} (see Materials and Methods) with parameter values of $G_{max-fit}=17.09$ nS (2.06 nS pF $^{-1}$), voltage at half-peak activation $V_{1/2}=-13.6$ mV, steepness factor $k=7.34$ (JUL2017F; cell input capacitance $C_{in}=8.3$ pF). Corresponding data from a transverse arm fiber are provided in D and E (open circles, computed from records in Fig. 2D). Parameters for the solid (blue) sigmoid are $G_{max-fit}=3.05$ nS (0.26 nS pF $^{-1}$), $V_{1/2}=-11.1$ mV, $k=6.88$. For this arm fiber, $G_{max-slope}=0.26$ nS pF $^{-1}$ and $V_{Na}=14.4$ mV (JUL2117A; $C_{in}=11.7$ pF).

Maximum G_{Na} density computed from all fibers was more than 10-fold larger in transverse muscle fibers from tentacles versus arms: 2.4 ± 0.9 versus 0.2 ± 0.2 nS pF $^{-1}$ (mean \pm s.d.) (Table S1). A more accurate assessment (6-fold difference) is probably provided by experiments that employed K-free solutions (480Na/220Na): 1.9 ± 0.5 versus 0.3 ± 0.1 nS pF $^{-1}$, respectively (Table S1). The difference in both cases is highly significant ($P < 0.0001$ by 2-tailed t -test). Parameters describing the shape of the $G_{Na}-V$ relationship ($V_{1/2}$ and k) were not significantly different in tentacles versus arms with the exception of $V_{1/2}$ in K-free solutions: -10.6 ± 2.5 versus -15.5 ± 3.2 mV ($P < 0.01$).

Kinetic features of activation and inactivation for I_{Na} were similar in tentacle and arm fibers, and deactivation kinetics during channel closing following a pulse were very rapid in both cases (time constant of ~ 100 μ s at -80 mV; not illustrated). Kinetic properties of I_{Na} from tentacle fibers were quantified by measuring the time to half-peak I_{Na} ($t_{1/2on}$), an activation time constant fitted to the final 25% of peak I_{Na} (τ_{on}) and an inactivation time constant ($\tau_{inactivation}$) as diagrammed in Fig. 4A. This allowed comparison of tentacle fiber data (filled symbols in Fig. 4A,B) with those from the same type of measurements made in giant fiber lobe neurons from the same species of squid at the same temperature (open symbols in Fig. 4; see Table S2 for details) (Gilly et al., 1997). I_{Na} in arm fibers was generally too small to permit detailed assessment of kinetic features.

Voltage dependence of G_{Na} inactivation was compared in tentacle and arm muscle fibers in the conventional way using depolarizing prepulses (-90 to -10 mV) followed by a test pulse to either 0 or $+40$ mV (Fig. 5A,B). The fraction of I_{Na} inactivated at each prepulse voltage (V_{pre}) was computed, and the relationship with V_{pre} was fitted with the same sigmoid equation used for quantifying the $G_{Na}-V$ relationship. Based on these fits for tentacle fibers, $V_{1/2}=-52.2 \pm 4.8$ and $k=5.1 \pm 0.8$ mV (mean \pm s.d.; $n=13$). Corresponding values for arms were $V_{1/2}=-55.7 \pm 3.1$ and $k=6.1 \pm 1.8$ mV ($n=5$), but the differences between arms and tentacles were not significant ($P=0.13$). These mean values of $V_{1/2}$ and k were used to compute the relationship between inactivation and V_{pre} for arm versus tentacle transverse fibers using Eqn 1, with the maximal fraction of inactivation set to 1.0 (Fig. 5C).

Voltage-dependent K conductance in transverse muscle fibers from tentacle versus arm

Every transverse muscle fiber showed voltage-dependent I_K that was large relative to I_{Na} , but tentacle fibers had a maximum G_K about 3-fold larger than that in arm fibers (7.4 ± 2.4 versus 2.5 ± 1.1 nS pF $^{-1}$; $P < 0.0001$). There were no significant differences in $V_{1/2}$ or k (Table S1). Kinetic properties of I_K , however, differed in the two fiber types. It is evident from inspection of records in Fig. 2B,C versus Fig. 2E,F that I_K in the arm fiber rises to its peak value more

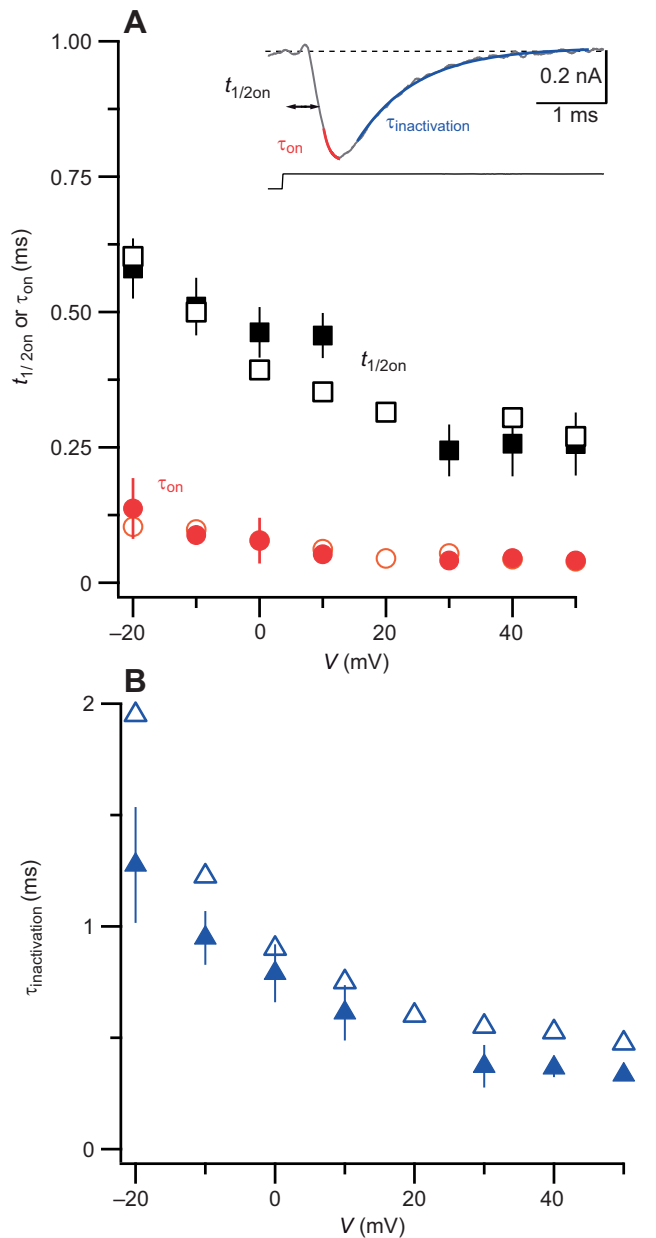


Fig. 4. Voltage dependence of I_{Na} kinetics. (A) The time to reach 50% of peak I_{Na} ($t_{1/2on}$; see inset) and the time constant (determined with an exponential fit) to the approach of I_{Na} over the final 25% (τ_{on}) were used to quantify kinetic features of I_{Na} in transverse tentacle fibers (mean \pm s.d., filled squares, $t_{1/2on}$; filled circles, τ_{on} ; see Table S2 for raw data and additional details). Open symbols represent measurements using the same procedures (i.e. prepulse and test-pulse voltages) with whole-cell patch-clamp recordings from cultured giant fiber lobe neurons ($n=2$) of the same species of squid at the same temperature (adapted from Gilly et al., 1997, and unpublished material). (B) Rate of inactivation ($\tau_{inactivation}$) was assessed by fitting an exponential to the decay of I_{Na} at a given voltage (see inset in A). Filled symbols represent data from transverse tentacle fibers (see Table S2 for raw data); open symbols represent data ($n=2$) from cultured giant fiber lobe neurons (Gilly et al., 1997).

rapidly than does I_K in the tentacle fiber at all of the illustrated voltages.

Quantitative comparison of I_K activation kinetics in the two fiber types is complicated by two major factors. First, I_{Na} to some extent temporally overlaps with I_K in both types of fiber, but the larger I_{Na} in tentacle fibers aggravates this problem. A prepulse procedure to

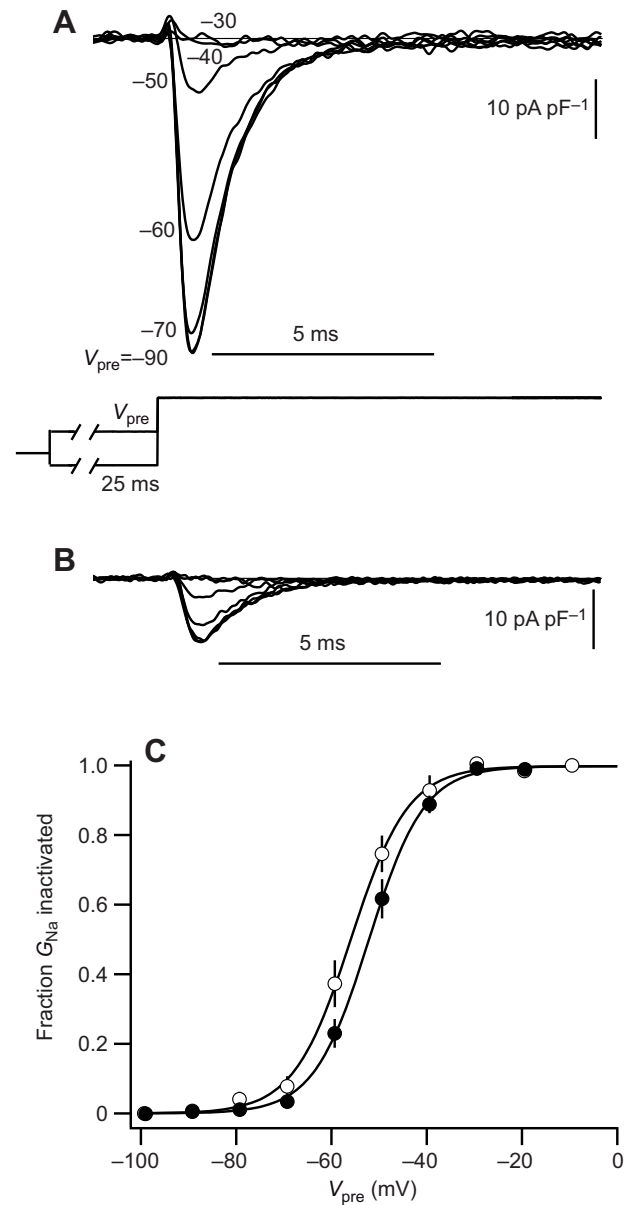


Fig. 5. Voltage dependence of I_{Na} inactivation in tentacle versus arm transverse muscle fibers. (A) I_{Na} in a tentacle fiber for a series of 25 ms prepulses to the indicated voltages (mV). I_{Na} is essentially completely inactivated by the prepulse (V_{pre}) to -30 mV (JUL2017G). (B) Records obtained with the same procedure for a transverse arm fiber (JUL2117D). (C) Fraction of I_{Na} inactivation versus V_{pre} . Solid symbols represent data from tentacle fibers (open symbols are for arm fibers; mean \pm s.d.). See Results for additional details and Table S2 for raw data.

inactivate I_{Na} also affects activation kinetics of I_K (see Fig. 2), although blocking I_{Na} with TTX reveals I_K in complete isolation (Fig. 6). Comparison of I_K from a tentacle fiber with that recorded from an arm fiber at the same voltage ($V_p=0$ mV) clearly shows that I_K , even in the presence of TTX, activates more slowly in the tentacle fibers. This qualitative difference was apparent at all voltages.

A second problem with quantifying I_K kinetics is that the currents are large enough to generate a significant R_s error essentially at all voltages >0 mV with the solutions employed. In several cases for command pulses to $+10$ mV, the maximum R_s error (at peak I_K) was <10 mV, and records from these experiments were analyzed in the

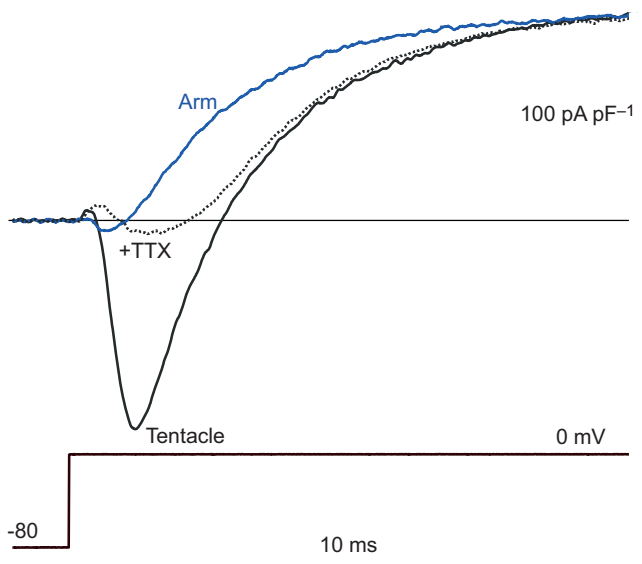


Fig. 6. Qualitative comparison of I_K activation kinetics in a tentacle versus arm fiber. I_K for a step to 0 mV is shown for a tentacle fiber in the absence (solid black trace) and presence (dotted trace) of 200 nmol l⁻¹ TTX to block I_{Na} and reveal I_K kinetics with minimal contamination. The trace recorded in TTX was scaled $\times 0.95$ (AUG1117C). The blue trace is I_K at 0 mV in an arm fiber scaled ($\times 0.90$) to the same maximum I_K (SEP0217A).

same manner as for I_{Na} activation kinetics (Fig. 4A). As indicated in Table S3, τ_{on} was significantly greater in tentacle versus arm fibers [3.5 ± 0.3 ms ($n=3$) versus 1.5 ± 0.8 ms ($n=9$); $P < 0.01$], but the lower value of $t_{1/2}$ in the same tentacle fibers was not significantly different from that in arm fibers (2.8 ± 0.3 versus 2.1 ± 0.7 ms; $P = 0.133$). Deactivation kinetics (channel closing, τ_{off}) at -70 mV did not differ significantly between the two types of transverse muscle fibers [5.7 ± 1.8 ms ($n=3$) versus 3.9 ± 1.8 ms ($n=7$); $P = 0.176$].

Another qualitative difference in voltage-dependent I_K in tentacle versus arm fibers was apparent in conjunction with inactivation properties. Long activating pulses (≥ 100 ms) with tentacle fibers revealed little or no inactivation of I_K at $+40$ mV (Fig. 7Ai), whereas I_K in arm fibers clearly inactivated during such pulses (Fig. 7Bi). Similarly, application of repetitive 10 ms pulses at a rate of ~ 30 Hz in tentacle fibers had little effect on the amplitude of I_K elicited by each pulse (Fig. 7Aii), but in arm fibers, I_K sequentially decreased with the same activating protocol (Fig. 7Bii). This latter procedure revealed that I_K declined over the four pulses by $6.2 \pm 6.9\%$ (mean \pm s.d.) in 6 tentacle fibers versus $34.6 \pm 15.2\%$ in 7 arm fibers, a highly significant difference ($P = 0.0015$).

Action potentials and G_{Na} in tentacles versus arms

Current-clamp recordings were carried out to test whether action potentials could be generated in either tentacle or arm fibers with the same solutions as those used for voltage-clamp experiments. After achieving the whole-cell configuration in voltage-clamp mode, a series of pulses was delivered to record I_{Na} and I_K , and then current clamp was enabled with the resting potential set manually to -70 mV. A series of depolarizing current pulses was then delivered, and the corresponding membrane potential changes were recorded.

Results from a transverse tentacle fiber are illustrated for voltage clamp (Fig. 8A) and for current clamp with long and short current pulses (Fig. 8Bi,ii). Inward I_{Na} was evident under voltage clamp, and an action potential was clearly generated with both current-pulse durations. Similar results were obtained in a total of 7 transverse tentacle fibers. Two other tentacle fibers showed a

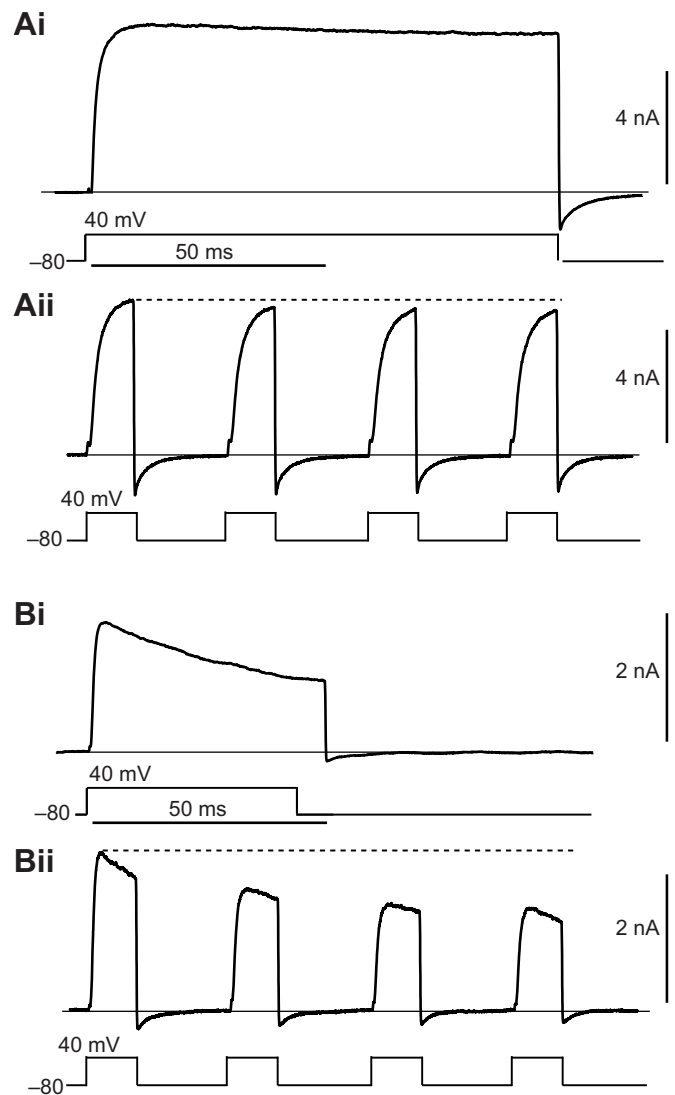


Fig. 7. Inactivation of I_K in tentacle versus arm fibers. (A) Inactivation of I_K in a tentacle fiber during a long activating pulse is minimal (Ai), and repetitive application of short pulses does not greatly affect the amplitude or time course of I_K (Aii) (MAY918D). (B) I_K in arm fibers inactivates during a long pulse (Bi), and repetitive pulses progressively reduce the amplitude of I_K (Bii) (Aug3018B).

detectable inflection in the positive-going voltage change but no obvious action potential.

In contrast, I_{Na} was essentially absent in a transverse arm fiber (Fig. 8C), and an action potential was not possible under current clamp (Fig. 8D). In this case the time course of the voltage change was due to activation of a delayed I_K that tends to drive the voltage towards V_K (~ -55 mV with the solutions used). Similar results were obtained in a total of four transverse arm fibers. An inflection point during the rising voltage waveform was not evident in any of these fibers.

A feature of action potentials in tentacle fibers is that they routinely were not as all-or-none as the classical action potential recorded from a squid giant axon or vertebrate muscle fiber. This is evident in Fig. 8B where the amplitude and rate of rise of the responses depended to some degree on stimulus amplitude. Typically, the rate of rise of an action potential varied at most over a 2-fold range in experiments of this type (Fig. 8Ei). This

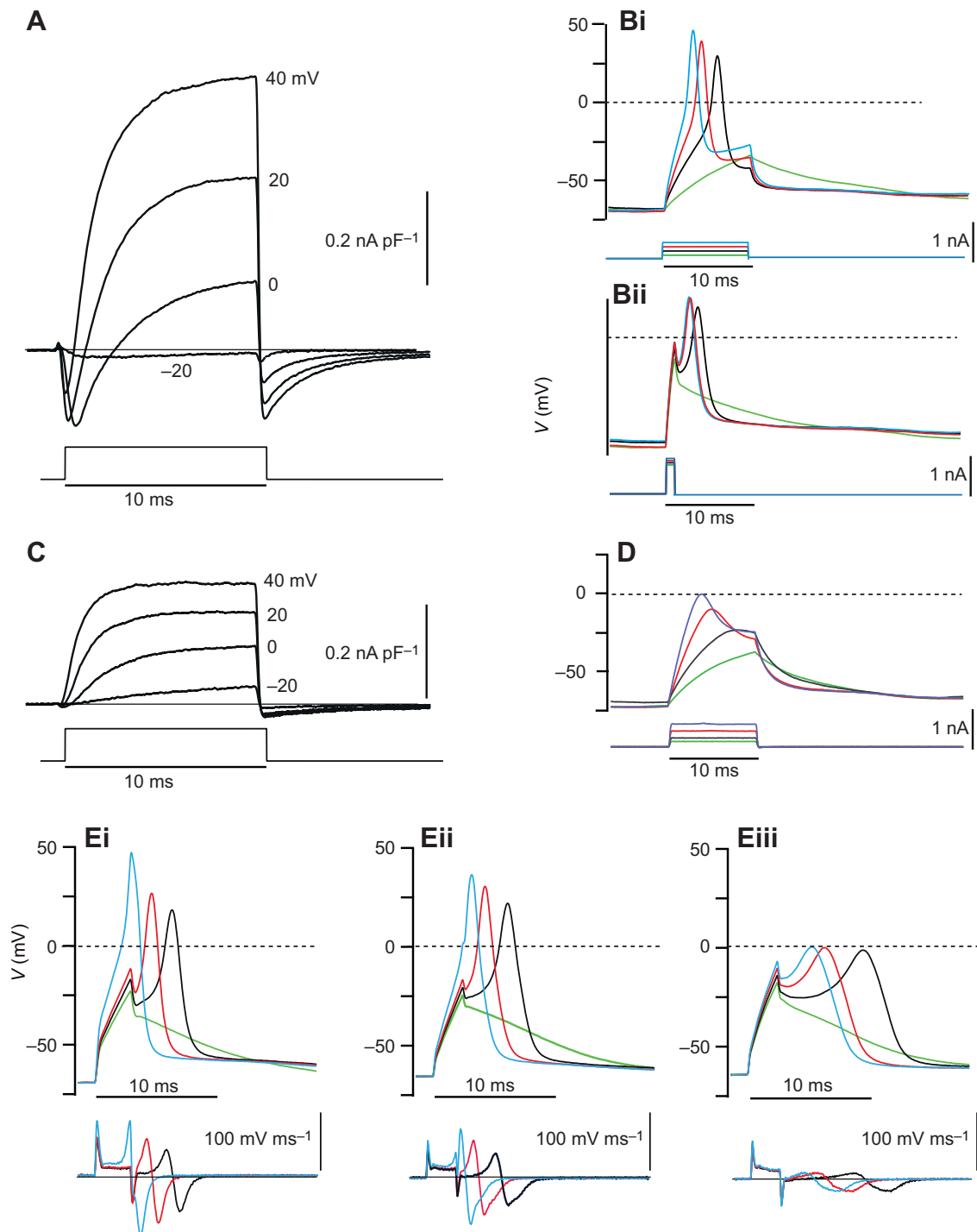


Fig. 8. Action potentials in transverse tentacle muscle fibers. (A) Voltage-clamp records of I_{Na} and I_K from a tentacle fiber were first obtained (AUG3117A). (B) Current-clamp recordings of membrane voltage changes in response to depolarizing current pulses were then recorded from the same fiber. Action potentials are evident with the three largest pulses for both long (Bi) and short (Bii) stimuli. (C,D) Analogous voltage-clamp (C) and current-clamp (D) recordings from an arm fiber (SEP0217A). There is little or no I_{Na} and no action potential is possible. The time course of voltage change is due to activation of voltage-dependent K channels. (E) Action potentials in tentacle fibers are graded in that amplitude and rate of rise depend on the stimulus strength. The time derivative of the voltage traces is given at the bottom. This feature was characteristic of tentacle fibers that had no detectable I_{Ca} (Ei; AUG3117B) as well as in a fiber that had a sizeable I_{Ca} (Eii; AUG3117C). In the latter fiber, it was possible to block I_{Na} with TTX and reveal a much slower and smaller action potential based on I_{Ca} (Eiii). This Ca-based response was not graded.

particular fiber had no detectable I_{Ca} as determined by a prepulse method to inactivate I_{Na} (not illustrated), and the graded nature of the response therefore appears to be associated with properties of G_{Na} and G_K .

Current-clamp experiments were also carried out in a tentacle fiber that had a significant I_{Ca} (0.3 nA peak I_{Ca} versus 4.0 nA peak I_{Na}), and the graded action potentials (Fig. 8Eii) were not distinguishable from those in fibers that lacked I_{Ca} (Fig. 8Ei).

Application of TTX (200 nmol l^{-1}) abolished the overshooting, fast action potential and revealed a much smaller and slower response, presumably due to Ca channel activation (Fig. 8Eiii). This response was essentially not graded in nature.

There was a clear relationship between the amount of G_{Na} and dV/dt rise in response to a depolarizing stimulus, and transverse fibers from arms and tentacles (Fig. 9, triangles) fell into two distinct groups. Correction for contamination by the stimulus (Fig. 9, squares; see Materials and Methods) did not alter the basic nature of this relationship. dV/dt fall (Fig. 9) showed a similar dependence on G_{Na} , because activation of voltage-dependent K channels is driven by the depolarization due to the G_{Na} increase that is responsible for the upstroke of the action potential. Again, arm fibers were clearly different from tentacle fibers.

Na channel mRNA in tentacles versus arms

Expression of mRNA encoding a voltage-gated sodium channel was assessed in tentacles and arms by *in situ* hybridization using an antisense probe to *D. pealeii* GFLN1, the lone voltage-dependent Na channel in this species. A sense probe to *X. laevis insm2* was used as a negative control. Low-magnification images of tentacle sections show a clear signal with the Na channel probe (Fig. 10A) as compared with the negative control probe (Fig. 10B). As anticipated, there was relatively intense labeling of Na channel mRNA in a region corresponding to the axial nerve cord (center of Fig. 10A), a structure that includes axon tracts as well as neuronal cell bodies.

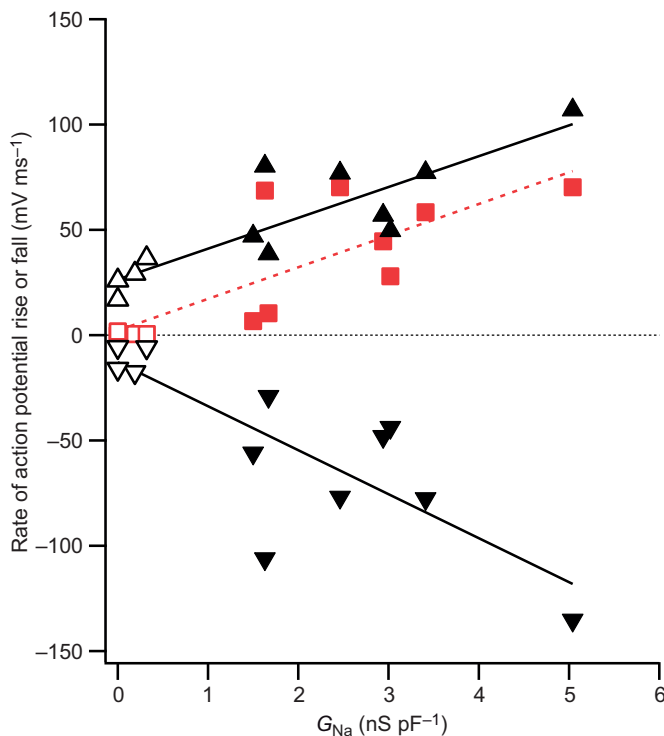


Fig. 9. Relationship between the rate of rise (and fall) of action potentials recorded under current-clamp with the amount of G_{Na} determined in the same fiber with voltage clamp. Filled symbols represent transverse tentacle fibers; open symbols represent arm fibers. The illustrated linear fits are highly significant: $r^2=0.746$, $P=0.0003$ for maximum rate of rise of action potentials (dV/dt rise; upward triangles, solid line, slope=14.63); $r^2=0.617$, $P=0.0025$ for dV/dt rise corrected for contamination by the stimulus (dV/dt rise* – see Table S4; squares, dashed line, slope=15.01); $r^2=0.651$, $P=0.0015$ for maximum rate of fall of action potentials (dV/dt fall; downward triangles, solid line, slope=-20.88).

Higher magnification images of the boxed regions in Fig. 10A,B show Na channel-specific signal in the transverse muscle fibers (Fig. 10C,D), with labeling being heaviest around nuclei. Similar sections from an arm showed no evidence of Na channel expression in muscle fibers (Fig. 10E,G) when compared with controls (Fig. 10F,H), although a clear Na channel signal was evident in the axial nerve cord (Fig. 10E). These data confirm Na channel mRNA expression in tentacle transverse muscle fibers, in consonance with the electrophysiological data. Sodium channel mRNA in arm transverse muscle fibers was apparently below the detection limit of our *in situ* hybridizations.

DISCUSSION

This paper clearly demonstrates that the transverse muscle fibers in the tentacles of squid have, on average, about 10-fold more G_{Na} than is found in the transverse arm fibers and that action potentials are possible in tentacle fibers but not in arm fibers. The difference in the level of G_{Na} density between the two fiber types was also reflected in the pattern of expression of mRNA encoding a voltage-dependent Na channel. Transverse tentacle fibers showed prominent expression of Na channel mRNA, whereas arm fibers had undetectably low levels of this transcript.

All of these features are thus consistent with the rapid extension of tentacles, a response that does not occur in the arms. A robust action potential in tentacle fibers, in comparison with the complete lack of any action potential in arm fibers, undoubtedly is responsible for the much greater twitch-to-tetanus ratio in tentacle versus arm transverse fibers. In a tentacle fiber, a few closely spaced action potentials would lead to maximal muscle fiber activation, whereas summation of excitatory postsynaptic potentials (EPSPs) over a longer time would be necessary in the arms.

Na conductance

Sodium channels expressed in transverse tentacle fibers are functionally similar to those expressed in squid giant axons as well as in cell bodies that form the giant axons (Gilly and Brismar, 1989; Gilly et al., 1997). Channels in all three preparations are blocked by $100\text{--}200 \text{ nmol l}^{-1}$ TTX, activation (and inactivation) show similar voltage dependence and kinetics, and deactivation (closing) kinetics are very fast. Fast activation kinetics at negative voltages clearly distinguish I_{Na} in these squid preparations from that found in neurons of gastropod mollusks (Gilly et al., 1997). The small I_{Na} in transverse arm fibers appears to have similar properties to that in tentacle fibers, but quantitative analysis of the voltage dependence of activation kinetics was not possible.

In consonance with the functional equivalence of Na channels in these preparations, mRNA encoding the relevant Na channels hybridized to the same probe for the GFLN1 sequence (Rosenthal and Gilly, 1993). Although another mRNA encoding a protein with overall sequence homology to a voltage-dependent Na channel has been identified in a closely related species of squid (Sato and Matsumoto, 1992), key residues in the voltage sensor and pore regions suggest that it encodes a channel with aberrant voltage sensitivity and cation selectivity, making it unlikely to encode the Na channels studied in this work or those in the squid axon system (Rosenthal and Gilly, 2003). Surprisingly, transcriptomes generated from nervous tissues of *D. pealeii* (Alon et al., 2015; Liscovitch-Brauer et al., 2017) and the genomes of the California two-spot octopus (*Octopus bimaculoides*; Albertin et al., 2015) and the Hawaiian bobtail squid (*Euprymna scolopes*; Belcaid et al., 2019) have revealed no additional Na_v homologs, suggesting that a single gene may encode voltage-dependent Na channels in cephalopods.

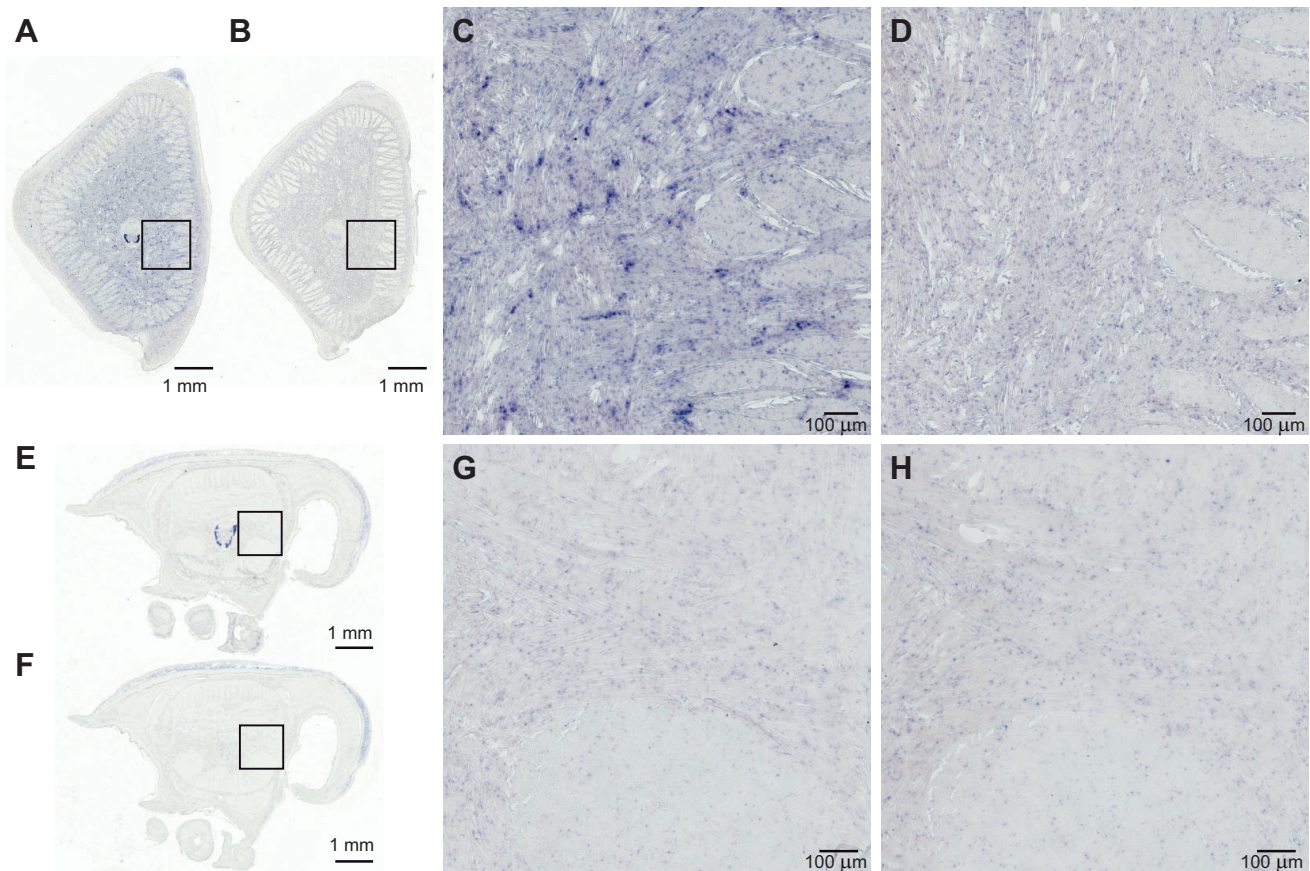


Fig. 10. *In situ* hybridization reveals Na channel mRNA expression in tentacle transverse muscle fibers. (A) A low-magnification image of a tentacle cross-section hybridized with an antisense Na channel probe shows labeling in the transverse muscle mass and axial nerve cord. (B) A low-magnification image of a tentacle cross-section hybridized with a negative control probe for *Xenopus laevis insm2* shows no labeling. (C,D) High-magnification views of the boxed regions in A and B, respectively, showing labeling in transverse muscle fibers (C) but not in the negative control (D). (E) A low-magnification image of an arm cross-section hybridized with the antisense Na channel probe shows no visible signal in the muscle mass but obvious labeling of the axial nerve cord. (F) A low-magnification image of an arm cross-section hybridized with a negative control probe for *X. laevis insm2* shows no labeling. (G,H) High-magnification views of the boxed regions in E and F, respectively.

Although functional properties of Na channels in transverse tentacle fibers are similar to those in the giant axon system, the density of Na channels, as estimated from G_{Na} , differs. In tentacle fibers, maximum G_{Na} was almost 5 nS pF^{-1} , whereas in giant-fiber-lobe neurons it can reach 10 nS pF^{-1} (Gilly et al., 1990), and in giant axons it is $\sim 20 \text{ nS pF}^{-1}$ (Hodgkin and Huxley, 1952). These differences correspond to proportional differences in the rate of action potential rise – a maximum of $50\text{--}100 \text{ mV ms}^{-1}$ in tentacle fibers (this study) versus an average of $374 \pm 35 \text{ mV ms}^{-1}$ (mean \pm s.d.; $n=4$) in giant axons of the same squid species at the same temperature (W.F.G., unpublished data). This result is expected based on the relationship between the rate of voltage (V) rise and the current (I) that discharges the membrane capacitance (C) during an action potential ($I = -CdV/dt$).

K conductance

Although Na channels are responsible for generating an action potential, voltage-dependent K channels are also important. Steady-state voltage dependence of G_K was similar in tentacles and arms, but G_K density in tentacles was ~ 3 -fold higher. We found that activation of I_K at a given voltage in tentacle fibers was slower than that in arm fibers. This feature would favor action potential generation in tentacle fibers, because the explosive nature of an action potential arises from the fact that I_{Na} activates much more

rapidly than does I_K . If the two processes overlap temporally, the situation is more complicated, and excitability is suppressed.

We also found that features of inactivation clearly distinguish G_K in arm fibers from that in tentacles. Inactivation was much more pronounced and rapid in arm fibers, and inactivation built up during repeated pulses. The phenomenon is similar to the classic ‘cumulative inactivation’ in molluscan neurons (Aldrich et al., 1979) that has subsequently been identified for many types of K channels (Bähring et al., 2012). Cumulative inactivation in the arm fibers would tend to increase excitability during repetitive neural stimulation. Although an action potential might never be possible with the 10-fold smaller G_{Na} in arm versus tentacle fibers (see Fig. 9), cumulative inactivation in arm fibers would be expected to lead to facilitation of EPSP amplitude during repetitive firing in motor axons. This mechanism could be important in regulating the output of transverse arm fibers by stimulus frequency.

Graded excitability in tentacle fibers

An interesting feature of excitability in tentacle fibers is that action potentials do not appear to be strictly ‘all or nothing’ like those in squid giant axon or vertebrate muscle fibers. This is apparent in the response of individual cells in which the amplitude and rate of rise of the action potential depended somewhat on stimulus strength (Fig. 8B,Ei,Eii). The relationship between the maximum rate of rise

(and fall) of the action potential and G_{Na} suggests that individual fibers differ in this regard. Fibers with G_{Na} at the upper end of the range had the largest and fastest action potentials, but they also showed the most graded nature of the response. This was true for both short and long stimulating pulses. Fibers in the middle of the G_{Na} range showed slower spikes, and the response was less graded. These fibers tended to not make action potentials with stimulating pulses of less than 5 ms duration. Fibers with little G_{Na} showed an inflection in the rising voltage change but nothing that qualitatively looked like an action potential.

Graded excitability in transverse tentacle fibers thus appears to be associated primarily with differences in the amount of G_{Na} present. This feature could in principle grade action potential amplitude rate of rise in response to variation in the amplitude of EPSPs due to motor-axon activity. Fibers with high G_{Na} have a wider scope of excitability to exploit, and action potential upstroke velocities appear to vary over a 2-fold range. This feature may enable peripheral elements, specifically muscle fibers, to play a significant role in coordinating neuromuscular outputs. A similar conclusion has been reached in a recent analysis of excitability of arm muscle fibers of an octopus, but in this case excitability is based on repetitive firing of Ca-based action potentials (Nesher et al., 2019).

Although graded excitability is a nearly universal feature of many types of invertebrate muscle, to our knowledge it has previously been associated only with Ca channels (Hoyle, 1969; Zachar, 1971). In most cases Ca and K channels have similar activation properties, and the temporal overlap of Ca influx and K efflux prohibits all-or-none responses. Crustacean muscle fibers are most well known for graded electrical responses that can be converted to all-or-none by blocking K channels (Fatt and Ginsborg, 1958; Hagiwara et al., 1964). Muscle fibers in octopus arms, however, do show Ca-based action potentials without blocking K channels, and gradation of muscular output appears to depend on firing frequency (Nesher et al., 2019).

Transverse tentacle fibers in squid provide an interesting exception to this rule. Although the gradation in action potential rate-of-rise is only 2-fold, this could provide additional control over feeding behavior *in vivo* that depends on a properly aimed and timed tentacular strike. Circular muscle fibers of squid mantle that are responsible for powerful jet propulsion also show a range of G_{Na} that is almost identical to that seen in tentacle fibers (2–6 nS pF⁻¹; Gilly et al., 1996). Although action potentials were not recorded in the cited study, results of the present paper suggest that graded Na-based action potentials in circular muscle fibers may be a feature of squid mantle muscle as well. A control mechanism of this sort may prove to be fairly widespread in the soft-bodied and highly mobile cephalopod mollusks.

Acknowledgements

We thank O. V. Drake and L. Gregg for assistance with animal maintenance and preparation of isolated muscle fibers, B. Burford for squid collection, S. Whitfield for help with graphics, P. D. Daniel for general assistance with the patch-clamp experiments, B. Hochner for helpful discussions, and J. S. Gillis for helpful advice on *in situ* hybridization techniques.

Competing interests

The authors declare no competing or financial interests.

Author contributions

Conceptualization: W.F.G., W.M.K.; Methodology: W.F.G., J.J.C.R., W.M.K.; Software: W.F.G.; Validation: W.F.G., W.M.K.; Formal analysis: W.F.G., W.M.K.; Investigation: W.F.G., C.R., W.M.K.; Resources: W.F.G., J.J.C.R., W.M.K.; Data curation: W.F.G., W.M.K.; Writing - original draft: W.F.G., C.R., J.J.C.R., W.M.K.; Writing - review & editing: W.F.G., J.J.C.R., W.M.K.; Visualization: W.F.G., C.R., J.J.C.R., W.M.K.; Supervision: W.F.G., J.J.C.R., W.M.K.; Project administration: W.F.G., W.M.K.; Funding acquisition: W.F.G., J.J.C.R., W.M.K.

Funding

This work was supported by the National Science Foundation (IOS 1557754 to W.F.G. and IOS 0951067 to W.M.K.).

Data availability

Raw electrophysiological time-series data (Axon binary files) used in the preparation of displayed figures are available from figshare (https://figshare.com/articles/Specialization_for_rapid_excitation_in_fast_squid_tentacle_muscle_involves_action_potentials_absent_in_slow_arm_muscle/11717355) along with relevant metadata as a Microsoft Excel file. Axon pCLAMP 9-Clampfit software should be used to view and analyze these files (http://mdc.custhelp.com/app/answers/detail/a_id/18826/~/axon%E2%84%A2-pclamp%C2%AE-9-electrophysiology-data-acquisition-%26-analysis-software-download).

Supplementary information

Supplementary information available online at <http://jeb.biologists.org/lookup/doi/10.1242/jeb.218081.supplemental>

References

- Albertin, C. B., Simakov, O., Mitros, T., Wang, Z. Y., Pungor, J. R., Edsinger-Gonzales, E., Brenner, S., Ragsdale, C. W. and Rokhsar, D. S. (2015). The octopus genome and the evolution of cephalopod neural and morphological novelties. *Nature* **524**, 220–224. doi:10.1038/nature14668
- Aldrich, R. W., Jr., Getting, P. A. and Thompson, S. H. (1979). Inactivation of delayed outward current in molluscan neurone somata. *J. Physiol.* **291**, 507–530. doi:10.1113/jphysiol.1979.sp012828
- Alon, S., Garrett, S. C., Levanon, E. Y., Olson, S., Graveley, B. R., Rosenthal, J. J. and Eisenberg, E. (2015). The majority of transcripts in the squid nervous system are extensively recoded by A-to-I RNA editing. *eLife* **4**, 613. doi:10.7554/eLife.05198
- Armstrong, C. M. and Gilly, W. F. (1992). Access resistance and space-clamp problems associated with whole-cell patch clamping. *Methods Enzymol.* **207**, 100–122. doi:10.1016/0076-6879(92)07007-B
- Bähring, R., Barghaan, J., Westemeier, R. and Wollberg, J. (2012). Voltage sensor inactivation in potassium channels. *Front. Pharmacol.* **3**, 1–8. doi:10.3389/fphar.2012.00100
- Belcaid, M., Casaburi, G., McNulty, S. J., Schmidbaur, H., Suria, A. M., Moriano-Gutierrez, S., Pankey, M. S., Oakley, T. H., Kremer, N., Koch, E. J. et al. (2019). Symbiotic organs shaped by distinct modes of genome evolution in cephalopods. *Proc. Natl. Acad. Sci. USA* **116**, 3030–3035. doi:10.1073/pnas.1817322116
- Fatt, P. and Ginsborg, B. L. (1958). The ionic requirements for the production of action potentials in crustacean muscle fibres. *J. Physiol.* **142**, 516–543. doi:10.1113/jphysiol.1958.sp006034
- Gilly, W. F. and Brismar, T. (1989). Properties of appropriately and inappropriately expressed sodium channels in squid giant axon and its somata. *J. Neurosci.* **9**, 1362–1374. doi:10.1523/JNEUROSCI.09-04-01362.1989
- Gilly, W. F., Lucero, M. T. and Horrigan, F. H. (1990). Control of the spatial distribution of sodium channels in giant fiber lobe neurons of the squid. *Neuron* **5**, 663–674. doi:10.1016/0896-6273(90)90220-A
- Gilly, W. F., Preuss, T. and McFarlane, M. B. (1996). All-or-none contraction and sodium channels in a subset of circular muscle fibers of squid mantle. *Biol. Bull.* **191**, 337–340. doi:10.2307/1543006
- Gilly, W. F., Gillette, R. and McFarlane, M. (1997). Fast and slow activation kinetics of voltage-gated sodium channels in molluscan neurons. *J. Neurophysiol.* **77**, 2373–2384. doi:10.1152/jn.1997.77.5.2373
- Hagiwara, S., Chichibu, S. and Naka, K. (1964). The effects of various ions on resting and spike potentials of barnacle muscle fibers. *J. Gen. Physiol.* **48**, 163–179. doi:10.1085/jgp.48.1.163
- Hodgkin, A. L. and Huxley, A. F. (1952). Currents carried by sodium and potassium ions through the membrane of the giant axon of *Loligo*. *J. Physiol.* **116**, 449–472. doi:10.1113/jphysiol.1952.sp004717
- Hoyle, G. (1969). Comparative aspects of muscle. *Annu. Rev. Physiol.* **31**, 43–84. doi:10.1146/annurev.ph.31.030169.000355
- Kier, W. M. (1982). The functional morphology of the musculature of squid (Loliginidae) arms and tentacles. *J. Morphol.* **172**, 179–192. doi:10.1002/jmor.1051720205
- Kier, W. M. (1985). The musculature of squid arms and tentacles: ultrastructural evidence for functional differences. *J. Morphol.* **185**, 223–239. doi:10.1002/jmor.1051850208
- Kier, W. M. (1991). Squid cross-striated muscle: the evolution of a specialized muscle fiber type. *Bull. Mar. Sci.* **49**, 389–403.
- Kier, W. M. (1996). Muscle development in squid: ultrastructural differentiation of a specialized muscle fiber type. *J. Morphol.* **229**, 271–288. doi:10.1002/(SICI)1097-4687(199609)229:3<271::AID-JMOR3>3.0.CO;2-1
- Kier, W. M. (2016). The musculature of coleoid cephalopod arms and tentacles. *Front. Cell Dev. Biol.* **4**, 10. doi:10.3389/fcell.2016.00010

- Kier, W. M. and Curtin, N. A.** (2002). Fast muscle in squid (*Loligo pealeii*): contractile properties of a specialized muscle fibre type. *J. Exp. Biol.* **205**, 1907-1916.
- Kier, W. M. and Schachat, F. H.** (1992). Biochemical comparison of fast- and slow-contracting squid muscle. *J. Exp. Biol.* **168**, 41-56.
- Kier, W. M. and Schachat, F. H.** (2008). Muscle specialization in the squid motor system. *J. Exp. Biol.* **211**, 164-169. doi:10.1242/jeb.008144
- Kier, W. M. and Van Leeuwen, J. L.** (1997). A kinematic analysis of tentacle extension in the squid *Loligo pealeii*. *J. Exp. Biol.* **200**, 41-53.
- Liscovitch-Brauer, N., Alon, S., Porath, H. T., Elstein, B., Unger, R., Ziv, T., Admon, A., Levanon, E. Y., Rosenthal, J. J. C. and Eisenberg, E.** (2017). Trade-off between transcriptome plasticity and genome evolution in cephalopods. *Cell* **169**, 191-202. doi:10.1016/j.cell.2017.03.025
- O'Neill, P., McCole, R. B. and Baker, C. V. H.** (2007). A molecular analysis of neurogenic placode and cranial sensory ganglion development in the shark, *Scyliorhinus canicula*. *Dev. Biol.* **304**, 156-181. doi:10.1016/j.ydbio.2006.12.029
- Nesher, N., Maiole, F., Shomrat, T., Hochner, B. and Zullo, L.** (2019). From synaptic input to muscle contraction: arm muscle cells of *Octopus vulgaris* show unique neuromuscular junction and excitation-contraction coupling properties. *Proc. R. Soc. B* **286**, 20191278. doi:10.1098/rspb.2019.1278
- Patek, S. N.** (2015). The most powerful movements in biology. *Am. Sci.* **103**, 330-337. doi:10.1511/2015.116.330
- Rokni, D. and Hochner, B.** (2002). Ionic currents underlying fast action potentials in the obliquely striated muscle cells of the octopus arm. *J. Neurophysiol.* **88**, 3386-3397. doi:10.1152/jn.00383.2002
- Rosenthal, J. J. C. and Gilly, W. F.** (1993). Amino acid sequence of a putative sodium channel expressed in the giant axon of the squid, *Loligo opalescens*. *Proc. Natl. Acad. Sci. USA* **90**, 10026-10030. doi:10.1073/pnas.90.21.10026
- Rosenthal, J. J. C. and Gilly, W. F.** (2003). Identified ion channels in the squid nervous system. *Neurosignals* **12**, 126-141. doi:10.1159/000072160
- Sato, C. and Matsumoto, G.** (1992). Primary structure of squid sodium channel deduced from the complementary DNA sequence. *Biochem. Biophys. Res. Commun.* **186**, 61-68. doi:10.1016/S0006-291X(05)80775-2
- Schindelin, J., Arganda-Carreras, I., Frise, E., Kaynig, V., Longair, M., Pietzsch, T., Preibisch, S., Rueden, C., Saalfeld, S., Schmid, B. et al.** (2012). Fiji: an open-source platform for biological-image analysis. *Nat. Methods* **9**, 676-682. doi:10.1038/nmeth.2019
- Shaffer, J. F. and Kier, W. M.** (2012). Muscular tissues of the squid *Doryteuthis pealeii* express identical myosin heavy chain isoforms: an alternative mechanism for tuning contractile speed. *J. Exp. Biol.* **215**, 239-246. doi:10.1242/jeb.064055
- Shaffer, J. F. and Kier, W. M.** (2016). Tuning of shortening speed in coleoid cephalopod muscle: no evidence for tissue-specific muscle myosin heavy chain isoforms. *Invert. Biol.* **135**, 3-12. doi:10.1111/ivb.12111
- Van Leeuwen, J. L. and Kier, W. M.** (1997). Functional design of tentacles in squid: linking sarcomere ultrastructure to gross morphological dynamics. *Phil. Trans. R. Soc. Lond. B* **352**, 551-571. doi:10.1098/rstb.1997.0038
- Zachar, J.** (1971). *Electrogenesis and Contractility in Skeletal Muscle Cells*. Baltimore, MD: Univ. Park Press.